Considerations for precast concrete girder end regions with large-diameter strands

Kent A. Harries, Tianqiao Liu, Bahram M. Shahrooz, Richard A. Miller, and Reid W. Castrodale

- Strand debonding patterns and prestress transfer practices can result in local stresses at prestressed girder ends.
- This article presents a numerical and analytic study of various single-webbed prestressed concrete girder shapes for which large amounts of prestressing are necessitated.
- Methods are recommended to release prestressing strands that reduce the effect of portions of the flanges peeling away from the web.

In previous work, the authors[1–3] and others[4,5] have addressed several issues affecting the end regions of prestressed concrete bridge girders, especially those with high pretensioning forces requiring a large degree of strand debonding to meet concrete stress limits at pretension transfer. Harries, Shahrooz, Ball, et al.[2] presents a detailed strut-and-tie modeling approach (**Fig. 1**) intended to assess transverse confinement reinforcement requirements in the bottom flange of single-webbed girders at the girder end (Fig. 1 middle). These requirements are an ultimate limit state and are intended to maintain sufficient strand anchorage to resist the high tension demands near a girder support affected by the presence of shear (article 5.7.3.5 in the American Association of State Highway and Transportation Officials' *AASHTO LRFD Bridge Design Specifications*)[6]. The strut-and-tie modeling approach was used to establish guidelines for the preferred strand and strand partial debonding patterns for single-web flanged girders proposed by Shahrooz et al.[3] these guidelines include the following recommendations (Fig. 1):

1. No more than 50% of the bottom row of strands should be debonded.
2. The outermost strands in all rows within the full-width section of the flange should remain bonded.
3. Except for the outermost strands, strands further from the section centerline should be debonded, preferentially to those nearer the centerline.

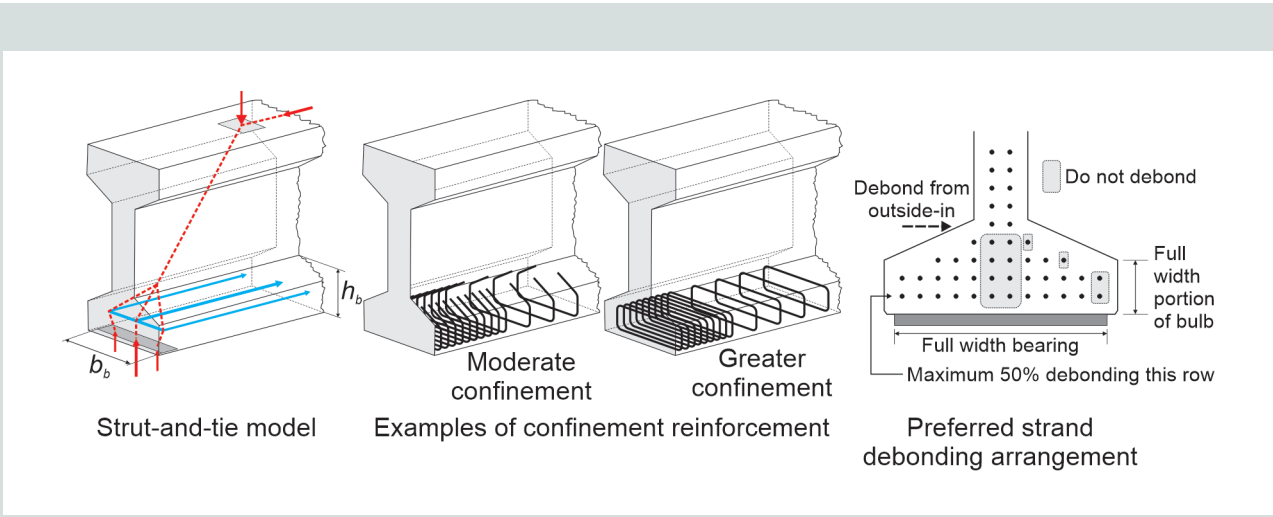

Figure 1. Single-web girder end region behavior and details.

4. Strands falling within the web width should remain bonded.

5. Debonded strands should be symmetrically distributed about the centerline of the cross section.

6. Full-flange-width bearing (or an embedded steel sole plate) should be provided at supports.

Recommendations 1 and 2 maximize prestress force at the concrete surface to limit cracking and ensure durability. Although recommendation 3 does not explicitly indicate that it is preferable to locate as many bonded strands within the web width as possible, this preference becomes apparent when the strut-and-tie modeling approach is applied. Strands falling within the web width do not contribute to the transverse tie force that must be developed (Harries et al.[2]).

A study by Harries, Shahrooz, Ball et al.[1] focused on extending the achievable spans of standard precast concrete girder shapes using a combination of high-strength concrete and 0.7 in. (17.8 mm) diameter strand in place of industry-standard 0.6 or 0.5 in. (15.2 or 12.7 mm) diameter strand. The greater pretension forces made possible through the use of larger strand required greater amounts of debonding (and harping) at girder ends to limit the concrete stresses at prestress transfer. The investigators conducted a parametric study of 448 single-web girder designs. Strand debonding patterns were based on the recommendations noted earlier to minimize the transverse confinement tie force required. All designs were deemed constructable, but some resulted in relatively congested girder end regions. The design case with the greatest confinement requirement—a University of Nebraska NU 2000 (79 in.) girder with 0.7 in. diameter strands designed to span 56.4 m (185 ft)—required confining reinforcement capable of resisting 1.7 kN/m (9.8 kip/in.) at the girder end. This tie force can be resisted by no. 3 (10M) hoops at 32 mm (1.25 in.), which violates the minimum bar spacing requirements in the AASHTO LRFD specifications; those requirements are no. 4 (13M) hoops at 57 mm (2.25 in.) or no. 5 (16M) hoops at 95 mm (3.75 in.). Many design cases required no confinement reinforcement beyond the minimum no. 3 bars at 152 mm (6 in.) required by the AASHTO LRFD specifications.[6]

Regardless of the strand pattern recommendations described, nonoptimized patterns may arise. Similarly, the pretension transfer operation (that is, strand release) may not be uniform or symmetrical. Such effects could give rise to other behaviors at the girder end, which will be magnified by high pretension forces.

Ross[5] identified behaviors related to the patterns of bonded strands and patterns of strand release, both of which can result in eccentric prestress force prying (or peeling away) the regions of the flange extending from the web (**Fig. 2**). This behavior was observed only in girders in which bonded prestressing strands were placed as far from the web as possible and with no fully bonded strands in the web region (contrary to the previously noted recommendations 3 and 4).

Ross[5] investigated a 54 in. (1370 mm) Florida I-beam (FIB54) girder (specimen F in Fig. 2) in which 20 of the 44 (45%) 0.6 in. (15.2 mm) diameter strands were debonded, with all debonded strands located near the centerline of the section (Fig. 2). The bearing width of 813 mm (32.0 in.) was similar to the flange width of 965 mm (38.0 in.), and the flange was confined with five sets of four-legged no. 4 (13M) bars within 420 mm (16.5 in.) of the girder end. Despite the confinement provided, cracks indicative of lateral splitting (solid lines in Fig. 2) occurred upon strand release. When tested under load, the specimen behavior was dominated by further splitting (dashed lines in the Fig. 2 cracking diagram).

Similarly, Llanos et al.[4] reported extensive splitting cracks upon prestress transfer at the end of an AASHTO Type IV girder (specimen A2U1) that had a particularly poor strand

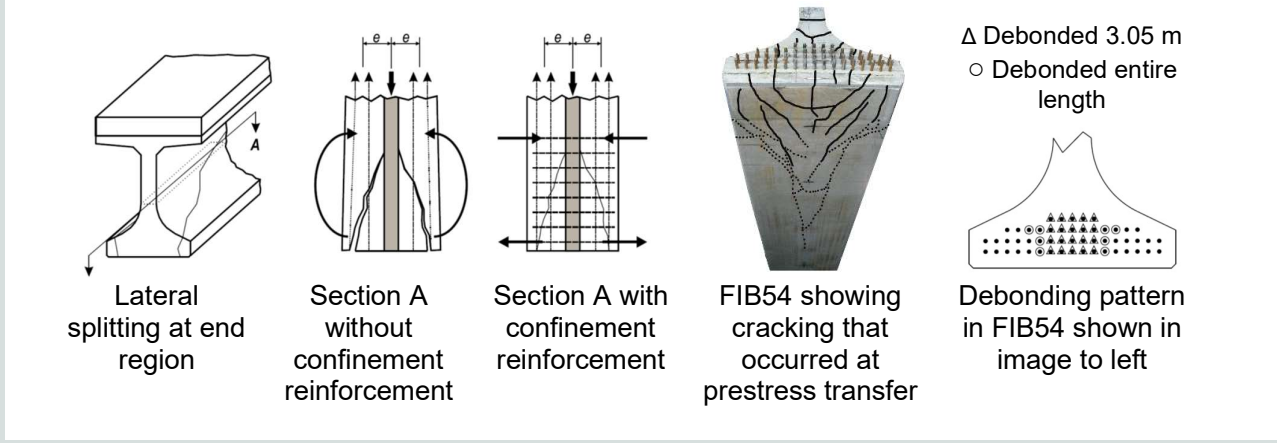

Figure 2. Lateral splitting behavior described by Ross. Note: FIB54 = 54 in. Florida I-beam. 1 m = 3.28 ft. Source: Reproduced by permission from Ross (2012).

debonding pattern (**Fig. 3**). Thirty-three straight 0.6 in. (15.2 mm) diameter strands, each stressed to $0.66f_{pu}$, (where f_{pu} is the ultimate tensile capacity of the strands) were provided. Of the 33 strands, 20 (61%) were debonded (middle of Fig. 3), with all debonded strands clustered in the web (contrary to recommendation 4). In addition, the bearing was only 406 mm (16 in.) wide, centered on the 660 mm (26 in.) wide flange, and did not extend beneath the fully bonded strands (contrary to recommendation 6). In this case, the compressive strut resulting from the application of a shear load was required to spread from the web to engage the outermost bonded strands and return inward to be reacted at the bearing pad.[2] This flow of force resulted in a transverse tension tie developing (Fig. 3), leading to the vertical cracks in Fig. 3. The girder had no confinement reinforcement in the flange. The outward thrust of the struts appears to have pushed off the concrete cover (Fig. 3), although this outcome could also represent the effect of lateral splitting.

Mechanistic modeling of effects of prestress transfer

The previous discussion of behavior and strut-and-tie modeling implicitly assumes a symmetrical arrangement of strand forces. During prestress transfer (release), this assumption may not be correct. Nonetheless, at prestress transfer, stresses and strains will typically remain in the elastic, uncracked range. When the stresses exceed those expected to cause cracking, serviceability and long-term durability are the primary concerns.

As described previously and shown in Fig. 2, Ross[5] identified several issues associated with prestress transfer. Ross went on

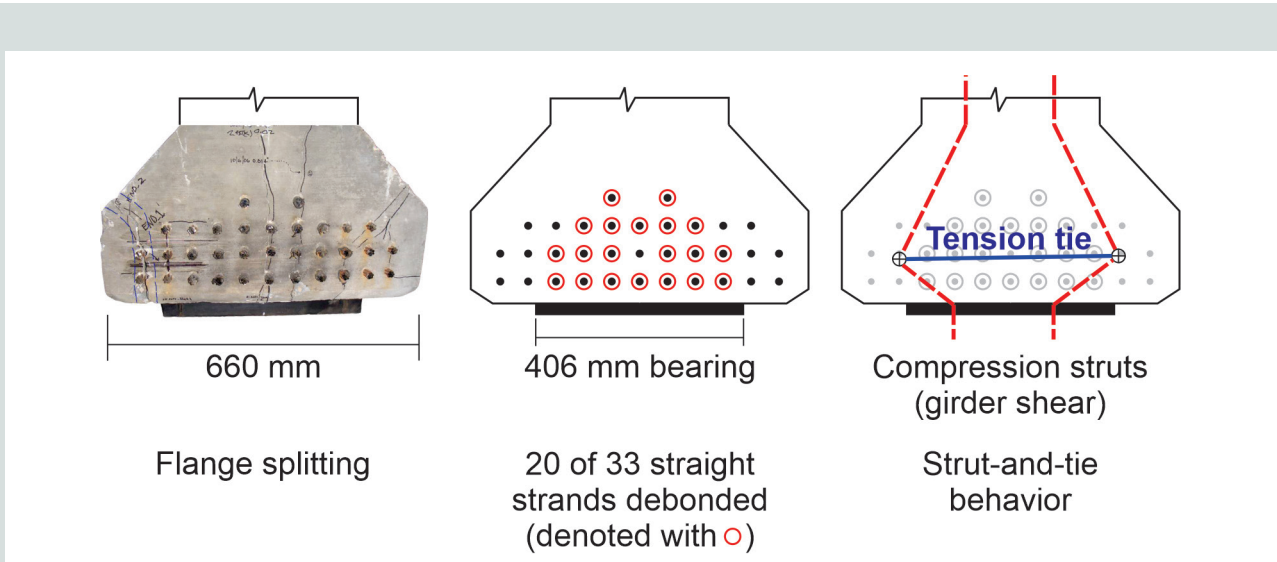

Figure 3. AASHTO Type IV girder end region behavior associated with poor strand debonding pattern. Note: 1 mm = 0.039 in. Flange-splitting source: Llanos et al. (2009).

to conduct a parametric study using the finite element method to investigate these issues using FIB-shaped girders. Ross drew the following conclusions for which the authors of the present study have provided commentary:

- "For [an outside-in] release sequence, the largest transverse tensile stresses during prestress transfer occur at the centerline of [the] section at the girder end. Centerline tension stresses are greatest when only the strands in the outer portion of the flange have been cut. Cutting of inner strands reduces this transverse tension."

Related to this finding, but considering a section away from the girder centerline:

- "During prestress transfer the maximum transverse tensile stress on an arbitrary vertical line through the bottom flange occurs when only the strands outboard (closer to edge) of the line have been cut. Cutting of strands along or inboard (closer to centerline) of a line relieve tensile stresses on that line. [For the FIB shapes considered,] transverse stresses at the end of the bottom flange are compressive after all strands have been cut."

- "Transverse stress and forces [at the girder end regions] are inversely proportional to strand transfer length. Thus, the greatest transverse effects occur in girders with the shortest transfer lengths." This illustrates the beneficial effect of debonding which shifts some of the total pretension force transfer away from the girder ends.

- "[Girder] self-weight reaction produces transverse tension forces in the bottom flange above the bearing." This effect was minor, and Ross concluded that it can be neglected for FIB shapes. It is primarily affected by the bearing width, with smaller widths and smaller ratios of bearing width to girder width resulting in higher transverse tension forces. It seems that the self-weight stress in Ross's study was calculated assuming a uniform reaction across the flange width. This assumption may be a theoretically critical case (indeed, it was adopted by Harries et al.[2] in the proposed strut-and-tie modeling analysis). However, a more realistic distribution (having greater stress beneath the web) reduces flange bending and affects transverse tension forces.

Based on these findings, Ross[5] proposed a simple mechanistic approach to investigate serviceability considerations associated with the transverse splitting (or peeling) behavior of the bottom flange associated with prestress transfer (**Fig. 4**). The transverse tension stress occurs across the critical sections A through G in the middle part of Fig. 4. Ross identified two critical conditions:

- maximum condition: the condition of maximum peeling stress at a section, which occurs when only the outboard strands are cut (whereas the strands at the section considered remain externally stressed)
- combined condition: the condition in which strands at the section considered are also cut

The stresses at the critical section are a function of the eccentric prestress forces during prestress transfer associated with the cutting sequence. Under the combined condition, the Hoyer effect[7,8] augments the splitting force near the girder end. Both conditions are described in the following sections. The critical cases described assume a worst-case strand release pattern in which all strands are cut (released) from the outside in. Any other release sequence reduces peeling stresses. Simultaneous release of all strands would result in no peeling stress (Fig. 4).

Peeling due to eccentric prestress force

The free body diagram in the middle part of Fig. 4 illustrates peeling stresses along any vertical plane (A through G) through the bottom flange.[5] The maximum transverse tension stress due to peeling is obtained from the conditions of moment equilibrium in the y-z plane (Fig. 4).

Equation (1) calculates the moment M due to releasing the number of bonded strands outboard of the section n_o defined by the depth of the bottom flange h_f (section C in Fig. 4).

$$M = n_o A_{ps} f_{ps} x_{po} \tag{1}$$

where

A_{ps} = area of single prestressing strand

f_{ps} = stress in prestressing strand

$A_{ps}f_{ps}$ = force in a single released strand; based on 10% losses; $A_{ps}f_{ps}$ is assumed to be $0.675A_{ps}f_{pu}$ in subsequent analyses

x_{po} = distance from the centroid of outboard strands to the vertical section defined by h_f

The internal resisting moment arm in the z direction is L_z (Fig. 4); therefore, the magnitude of the resisting tension T and compression C couple is calculated using Eq. (2).

$$T = C = M/L_z = n_o A_{ps} f_{ps} x_{po}/L_z \tag{2}$$

Finally, the tension stress is assumed to be distributed over the transfer length L_t (Fig. 4); therefore, Eq. (3) calculates the maximum transverse tension stress due to peeling f_p.

$$f_p = n_o A_{ps} f_{ps} x_{po}/0.5L_t(h_f - n_h d_b)L_z \tag{3}$$

where

d_b = strand diameter

n_h = number of strands with diameter d_b along the vertical section defined by h_f

Lengths L_t and L_z vary according to the number of cut strands, the shape of the cross section, and the section at which the

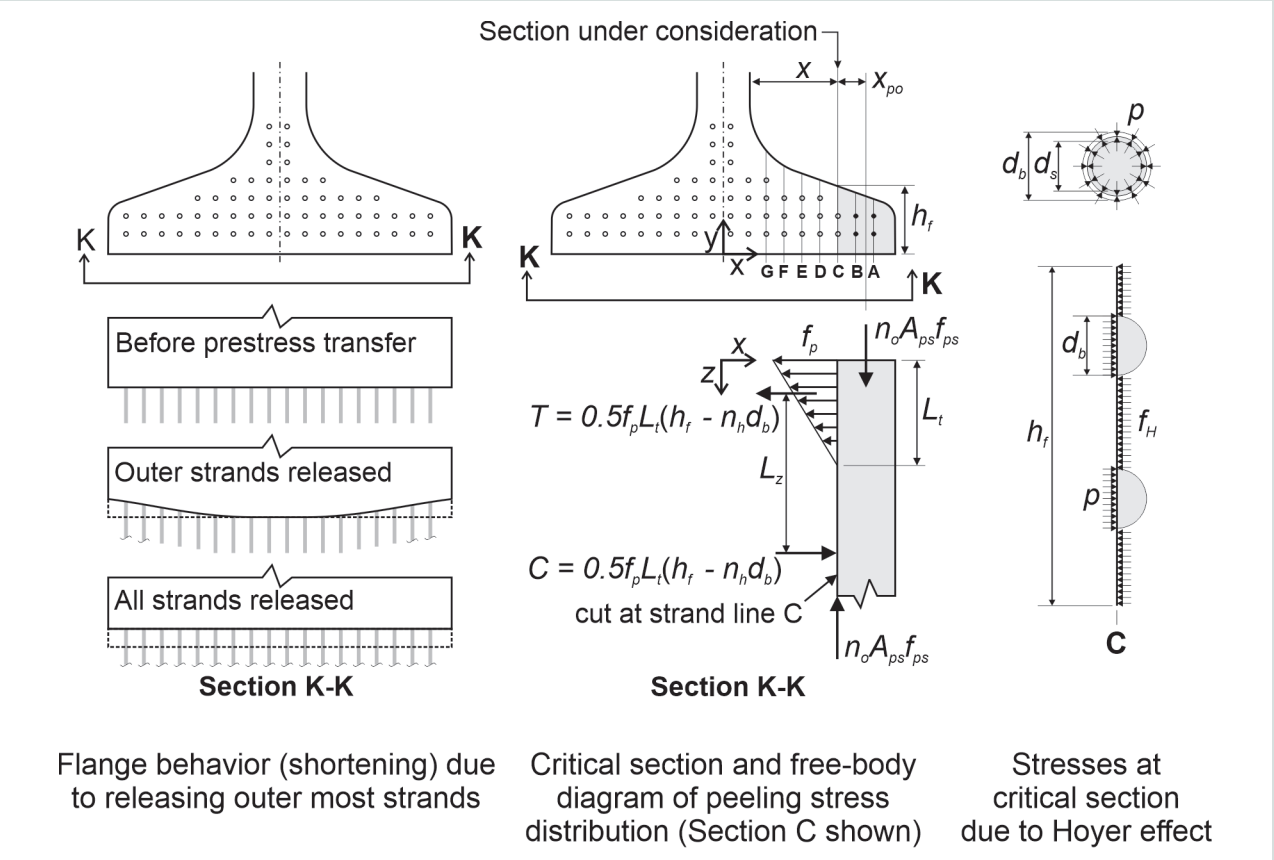

Figure 4. Peeling behavior at prestress transfer (after Ross). Note: A_{ps} = area of single prestressing strand; C = resisting compression; d_b = diameter of prestressing strand; d_s = stressed diameter of the prestressing strand; f_p = maximum transverse tension stress due to peeling; f_{ps} = stress in prestressing strand; h_f = height of bottom flange; L_t = transfer length; L_z = internal resisting moment arm in the z direction; n_h = number of strands with diameter d_b along the vertical section defined by h_f; n_o = number of bonded strands outboard of the section; p = radial pressure resulting from Hoyer effect; T = resisting tension; x = horizontal distance from the face of the web to the section considered; x_{po} = distance from the centroid of outboard strands to the vertical section defined by h_f.

calculation is made. For FIB girders, Ross[5] reported values of L_t equal to 254 mm (10.0 in.) and L_z equal to $1346h_f/x$ (where x is the horizontal distance from the face of the web to the section considered as shown in Fig. 4) and L_z equal to $914h_f/x$ for the maximum and combined conditions, respectively (L_z equals $53h_f/x$ and L_z equals $36h_f/x$, in inches respectively). These values are based on parametric study and experimental observation of FIB girders.

There are no known data for girders other than FIB shapes. Based on the mechanism in Fig. 4, peeling is analogous to transverse flexural behavior of the portion of the flange outboard of the section being considered. The moment of inertia of this portion of flange (with respect to the y-z plane) is a function of x_{po}^3 and h_f. The values of L_t and L_z are proportional to the moment of inertia; that is, a stiffer portion of the flange extending from the web reduces peeling stresses along the critical section. Therefore, in subsequent analyses, the values of L_t and L_z for other girder shapes have been estimated as those given by Ross[5] for FIB girders multiplied by the ratio $(x_{po}^3 h_f)_{shape}/(x_{po}^3 h_f)_{FIB}$.

Hoyer effect on peeling stresses

When a straight wire or tendon is placed in tension, its diameter decreases due to the Poisson effect. As the stress is relieved, the tendon, if unrestrained, returns to its original diameter (d_b in Fig. 4). Similarly, where the prestressing force has been developed (in the component beyond the transfer length), the tendon retains its stressed diameter (d_s in Fig. 4). Over the transfer length, as the tendon stress is reduced from the effective prestress f_{pe} at the transfer length (and beyond) to zero (at the free end of the component), the tendon attempts to return to its original diameter and, constrained by the concrete, radial forces develop along the concrete and tendon interface (Fig. 4). The resulting lateral expansion and development of radial forces improves the transfer of prestress force to the concrete; this is referred to as the Hoyer effect. Because of the geometry of seven-wire prestressing strand, the Hoyer effect for that type of strand is greater than the Poisson effect

alone. Values of strand dilation ratio υ_p as high as 0.40 have been reported by Briere et al,[8] which provides a complete discussion of the Hoyer effect of seven-wire prestressing strand.

In sound concrete, the Hoyer effect serves to improve the transfer of force between strand and concrete by enhancing the frictional component of bond.[9,10] However, when peeling behavior is considered, the concrete reaction to the Hoyer expansion of the strand results in additional tension along the critical section (Fig. 4). From equilibrium, the average transverse tension resulting from Hoyer expansion f_H is calculated using Eq. (4).

$$f_H = pn_{hb}d_b/(h_f - n_h d_b) \quad (4)$$

where

p = radial pressure resulting from Hoyer effect

n_{hb} = number of bonded strands

$h_f - n_h d_b$ = net area of concrete along the critical section

The maximum value of f_H is at the end of the girder, and f_H is zero at the strand transfer length and beyond. Equation (5) calculates the maximum value of p at z equal to zero.8,11

$$p = \frac{d_b - d_s}{\left(1-\upsilon_p\right)\frac{d_b}{E_p} + \left[\upsilon_c + \frac{\left(d_s/2\right)^2 + c^2}{\left(d_s/2\right)^2 - c^2}\right]\left(\frac{d_s}{E_c}\right)} \quad (5)$$

where

E_p = Young's modulus of prestressing strand

E_c = Young's modulus of confining concrete

υ_c = Poisson's ratio for concrete

c = concrete cover provided to the center of an outermost strand

For values of p other than at z equal to 0, Briere et al.[8] provides a complete derivation of Hoyer effect–induced stresses along the strand length and away from the strand-concrete interface.

Peeling stress calculations

There are two conditions for peeling. For the maximum condition, f_p is calculated by Eq. (1), and the strands at the section being considered are not released. The number of released strands is, therefore, all strands outboard of the section being considered n_o. For the combined condition, the same section is considered, but the strands at that section being considered are also released, thereby incrementing the peeling stress with the Hoyer-related stress f_H calculated by Eq. (2). In this condition, the number of released strands is $n_o + n_h$. The value of L_z is different for the different conditions;5 thus, f_p is not the same for each condition.

In the following analyses of peeling stress, transverse forces are calculated at vertical sections corresponding to the columns of strands of each girder; these sections are labeled, beginning with A at the outermost strands (Fig. 4). The analyses are worst-case scenarios because they assume an outside-in strand cutting sequence and that there are no debonded strands at the section considered (that is, n_{hb} equals n_h).

To make representative calculations, the following assumptions are made:

- E_c = 32.4 GPa (4700 ksi)
- E_p = 197 GPa (28,500 ksi)
- υ_c = 0.20
- υ_p = 0.34 for 0.6 in. (15 mm) diameter strands
- υ_p = 0.32 for 0.7 in. (18 mm) diameter strands[9,10]
- c = 51 mm (2.0 in.) for all girders other than FIB girders for which c = 76 mm (3.0 in.)
- $f_{ps} = 0.9 \times 0.75 f_{pu}$ = 1257 MPa (182.3 ksi)

Table 1 presents the values used for L_t and L_z, and prestressing with 0.6 and 0.7 in. (15 and 18 mm) diameter strands was considered. Peeling analyses were conducted for the following single-web girder shapes: FIB, AASHTO Type VI, PCI bulb tee, Ohio wide flange, NU section, and Washington State Department of Transportation (WSDOT) wide flange. The appendix provides tabulated results for all vertical sections through the flange (A through G in Fig. 4, which shows an NU section). Table 1 summarizes the resulting maximum stresses obtained for all girder shapes considered.

The tensile stress permitted by AASHTO[6] at prestress transfer is $0.50\sqrt{f'_{ci}}$ ($0.19\sqrt{f'_{ci}}$ in ksi), where f'_{ci} is compressive strength of concrete at the time of strand transfer. The value for f'_{ci} was assumed to be 55 MPa (8.0 ksi), which corresponds approximately to a specified 28-day concrete strength f'_c of 69 MPa (10 ksi).

In all cases, the peeling stress is greater for larger strand because each larger strand has a greater prestress force $A_{ps}f_{ps}$, and the area of concrete in tension is smaller for larger strand. These effects are only marginally mitigated by the trend for lower dilation ratios υ_p for larger strand diameter. The peeling stress is greatest for girders having shallow wide flanges reflecting the lower transverse bending stiffness of the region peeling away; the larger values of the lever arm x_{po} possible; and the smaller area resisting peeling stresses h_f. The poten-

Table 1. Summary of peeling stress analysis for I-shaped girders

Girder shape	Strand diameter, in.	L_t, mm	Maximum condition			Combined condition				
			L_z	f_p, MPa	At vertical plane	L_z	f_H, MPa	At vertical plane	$f_p + f_H$, MPa	At vertical plane
FIB	0.6	254	$1346h_f/x$	2.7	E	$914h_f/x$	2.6	C	6.9*	F
	0.7			3.7	E		4.1	C	10.2*	F
AASHTO VI	0.6	351	$1854h_f/x$	0.7	D	$1270h_f/x$	4.1	D	5.1*	F
	0.7			1.0	D		6.4	D	7.9*	F
PCI bulb tee	0.6	208	$1092h_f/x$	2.5	D	$762h_f/x$	3.7	E	7.1*	E
	0.7			3.5	D		5.7	E	10.5*	E
Ohio WF	0.6	165	$864h_f/x$	12.2*	G	$584h_f/x$	3.9	G	22.0*	G
	0.7			17.4*	G		6.1	G	32.0*	G
NU	0.6	201	$1067h_f/x$	9.2*	F	$711h_f/x$	3.6	G	16.5*	G
	0.7			12.9*	F		5.5	G	23.9*	G
WSDOT WF	0.6	196	$1041h_f/x$	9.3*	E	$711h_f/x$	3.4	G	16.8*	E
	0.7			13.2*	E		5.3	G	24.1*	E

Note: AASHTO = American Association of State Highway and Transportation Officials; FIB = Florida I-beam; f'_{ci} = concrete compressive strength at time of prestress transfer; f_H = average transverse tension resulting from Hoyer expansion; f_p = maximum transverse tension stress due to peeling; h_f = height of bottom flange; L_t = transfer length; L_z = internal resisting moment arm in the z direction; WF = wide flange; WSDOT = Washington State Department of Transportation. x = horizontal distance from the face of the web to the section considered. 1 in. = 25.4 mm; 1 mm = 0.039 in.; 1 MPa = 0.145 ksi.
*Tensile stress at prestress transfer exceeds $0.50\sqrt{f'_{ci}}$ in MPa ($0.19\sqrt{f'_{ci}}$ in ksi).

tially significant contribution of the Hoyer effect in pushing the portion of the flange extending from the web away from the web is evident.

The data presented in Table 1 represent the theoretical worst-case (and likely unrealistic) scenario in which the following is true:

- All strands in the flange are tensioned.
- No strands are debonded.
- There is an outside-in release sequence.

Deviation from this scenario reduces predicted stresses, as follows:

- Strand debonding, particularly in the recommended pattern of partial debonding (from the outside in) will mitigate Hoyer stresses f_H in proportion to the number of debonded strands at a vertical section: $n_h - n_{bh}$.
- Releasing or cutting strands in a more uniform manner, such as from the top down, will significantly mitigate peeling stresses by reducing no. Furthermore, the unreleased or uncut lower layer strands in a top-down release sequence restrain the peeling moment.
- For girders in which all strand locations in their bottom flange are used, it is unlikely that 0.6 in. (15.2 mm) diameter strand can be replaced one for one with 0.7 in. (17.8 mm) diameter strand.[1] Therefore, the increase in stress resulting from using 0.7 in. diameter strand may be only marginal, not proportional to the increased individual strand area but rather the sum of the strand area provided.

Finally, the stresses calculated are at the end face of the girder. Both Hoyer-related stresses f_H and peeling stresses f_p decrease (approximately) linearly with distance into the girder. Peeling stress f_p decreases to zero over the transfer length L_t (Fig. 4) whereas f_H decreases to zero at the real transfer length of the strand—typically about $30d_b$. While the results presented in Table 1 are worse-case scenarios, they do illustrate that peeling stresses associated with the strand-release pattern can be substantial and, if not considered, could cause cracking of the section, as seen in Fig. 2.

Finite element modeling of the strand-release sequence

The previous sections of this article establish the potential for peeling due to an improper strand-release sequence; Ohio wide-flange girders exhibited the greatest potential peeling stresses (Table 1). A series of finite element (FE) analyses were performed to validate the numerical study and extend the

analyses to release sequences that cannot be modeled using the analytic approach. A limitation of the FE analyses is that only peeling due to eccentric prestress force f_p is modeled; that is, the maximum peeling condition can be simulated. The FE model employs one-dimensional truss elements to model all reinforcing strands and bars; therefore, the Hoyer effect is not captured.

Full details, including extensive validation studies, of the full-girder-length FE model formulation using ATENA from Cervenka Consulting are reported in Shahrooz et al.[3] The authors subsequently used the same modeling approach successfully to investigate the full girder behavior and local behavior of prestressed concrete bridge girders.[1,10] In the analyses presented in this study, only the first step in modeling (that is, releasing the prestress strands) is considered. Material properties used for the models are consistent with those described earlier in this article. Initial prestress force f_{pi} was 1396 MPa (202.5 ksi) and transfer length L_t was consistent with the AASHTO LRFD specifications: $60d_b$ which equals 915 mm (36 in.) and 1067 mm (42 in.) for 0.6 and 0.7 in. (15.2 and 17.8 mm) diameter strands, respectively. Prestress losses upon transfer were determined within the FE model based on the bond slip model used by Shahrooz et al.:[3] in general, these losses are approximately 10% of the initial prestress force.

Table 2 shows the strand designations in the flange. Both 0.6 and 0.7 in. (15 mm and 18 mm) diameter strands were considered in the 28 strand-release sequences (Table 2). All strands were stressed to $0.75A_{ps}f_{ps}$, and each case represents only the strands that are indicated as being released. The remaining strands were assumed to still be stressed in the stressing bed. This condition potentially provides significant restraint at the beam end from the unreleased strands. In this model, this restraint is simplified by restraining uplift and horizontal (transverse) translation at the centerline of the beam at the beam support. Such restraint permits shortening of the beam, hogging (camber), sagging, and transverse bending to be captured by the model. In practice, this restraint would be complex and would vary based on the length of exposed strand between the girder end and stressing bulkhead; the release sequence itself because the girder will bend both horizontally and vertically, thereby affecting stress in unreleased strands; and perhaps other factors. Thus, the FE peeling analyses conducted are, like the numerical study, artificial. Although the absolute values reported should effectively illustrate trends in behavior, care should be taken in their interpretation.

To assess the theoretical maximum possible peeling stress, all strands are assumed to be present, and all strands (for the maximum peeling condition) are assumed to be bonded. Strand-release sequences B through H (Table 2) are the same as those described in the numerical study and are worse-case scenarios that model outside-in strand release from one side of the girder. Strand-release sequences I through N represent possible poor-case release sequences that combine top-down and outside-in sequences. The number 6 or 7 following the case designation indicates that the strand diameter is 0.6 or 0.7 in. (15.2 or 17.8 mm), respectively. Only transverse flange stresses are of interest in this study.

To model peeling stresses, which are a local effect, a half-span model of a 72 in. (1830 mm) deep Ohio wide-flange girder was used. The half span was made statically determinate with the following restraints intended to represent the restraint of a prestressed girder at prestress transfer:

- Vertical deflection is restrained across the entire width of the girder end; this restraint mimics the simple support of a prestressed girder at release when camber is expected. Uplift is not permitted at the support in this model (because the presence of unreleased strands would restrain uplift in the prestressing bed.
- Transverse (horizontal) deflection is restrained only at the centerline of the girder at the support; this boundary condition permits transverse bending of the girder due to eccentric strand release sequences.
- Longitudinal deflection is restrained at midspan of the beam, which is the typical restraint to represent a full-span model by its half span.

Finite element modeling of peeling stress results

For cases A-6 and A-7, all 60 strands were released simultaneously. **Figure 5** shows case A-7. As expected, flange stresses were symmetrical and peak tensile stresses are at the web and flange interface, related to splitting. This observation is consistent with the splitting reinforcement requirement of article 5.9.4.4.1 of the AASHTO LRFD specifications.

Cases B through H are the same as those described previously for Ohio wide-flange girders. n which strand release progresses from the outside of the section and progresses inward. Table 2 shows values from the analytical analysis for clarity and comparison. The stresses determined using FE modeling at the critical vertical sections are lower than those predicted by the analytical peeling analysis at the same locations (Table 2). Indeed, as the outside-in strand release moves from case B to case H, the stresses at the presumed critical planes (Fig. 4) become compressive. Examining the sequence from case B to case H (top row of Fig. 5), as the prestress force transferred to the flange increases, the girder behaves more like a beam bending about both principal axes. Ross[5] assumed a shear-like transfer of stress along the plane located at the x axis (**Fig. 6**) but neglected the transverse bending of the girder. Thus, the Ross model captures the behavior well for cases B and C, which have little transverse flexure. However, as more prestress force is transferred, weak-axis flexural behavior of the girder becomes dominant, resulting in more-complex behavior that is not captured by the simple model. It appears that the restraint provided by the unreleased strands has a significant effect on the stress transfer from the released strands. As noted earlier, this effect will vary and cannot be modeled except in a general sense. In addition, the maximum stress

Table 2. Strand-release sequences and maximum peeling stresses in Ohio wide flange girders

Case		Strands released	Finite element analysis results				Analytic results	
			Maximum transverse tension stress f_p, MPa	Occurs at vertical plane	Transverse tension stress f_p, MPa	At vertical plane	Maximum transverse tension stress f_p, MPa	Occurs at vertical plane
0.6 in. diameter strand	A-6	All strands	-0.21	H				
	B-6	A2	2.41	F	1.38	B	1.65	B
	C-6	All A and B	3.17	H	0.55	C	4.83	C
	D-6	All A–C	0.97	F	0.69	D	8.07	D
	E-6	All A–D	1.17	F	1.17	E	11.0	E
	F-6	All A– E	0.76	G/H	-3.24	F	12.1	F
	G-6	All A–F	0.76	H	-0.14	G	12.2	G
	H-6	All A–G	-0.97	G/H	-0.97	H	8.41	H
	I-6	All 4 and 5, C3, D3	-0.83	G/H				
	J-6	All 4 and 5, C3, D3, E3, F3	-0.62	G/H				
	K-6	All 3–5, A2, B2	0.34	G/H				
	L-6	All 3–5, A2, B2, C2, D2	1.38	G/H				
	M-6	All 2–5, B1, C1	1.24	G/H				
	N-6	All 2–5, B1, C1, D1, E1	1.31	H				
0.7 in. diameter strand	A-7	All strands	0.55	H				
	B-7	A2	2.41	F	1.24	B	2.34	B
	C-7	All A and B	2.96	H	0.41	C	6.90	C
	D-7	All A–C	0.34	H	-2.28	D	11.4	D
	E-7	All A–D	0.41	E	0.41	E	15.7	E
	F-7	All A–E	0.34	H	4.07	F	17.1	F
	G-7	All A–F	0.62	H	0.21	G	17.4	G
	H-7	All A–G	-1.72	G/H	-1.72	H	11.9	H
	I-7	All 4 and 5, C3, D3	-1.10	G/H				
	J-7	All 4 and 5, C3, D3, E3, F3	-0.34	G/H				
	K-7	All 3–5, A2, B2	-0.55	A				
	L-7	All 3–5, A2, B2, C2, D2	1.03	G/H				
	M-7	All 2–5, B1, C1	1.86	H				
	N-7	All 2–5, B1, C1, D1, E1	-0.07	G/H				

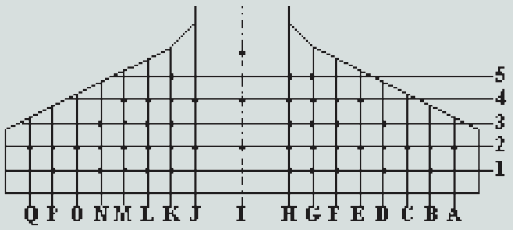

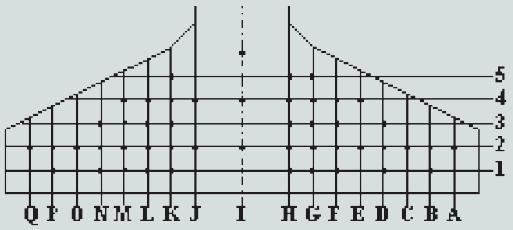

Note: f_p = maximum transverse tension stress due to peeling; 1 MPa = 0.145 ksi.

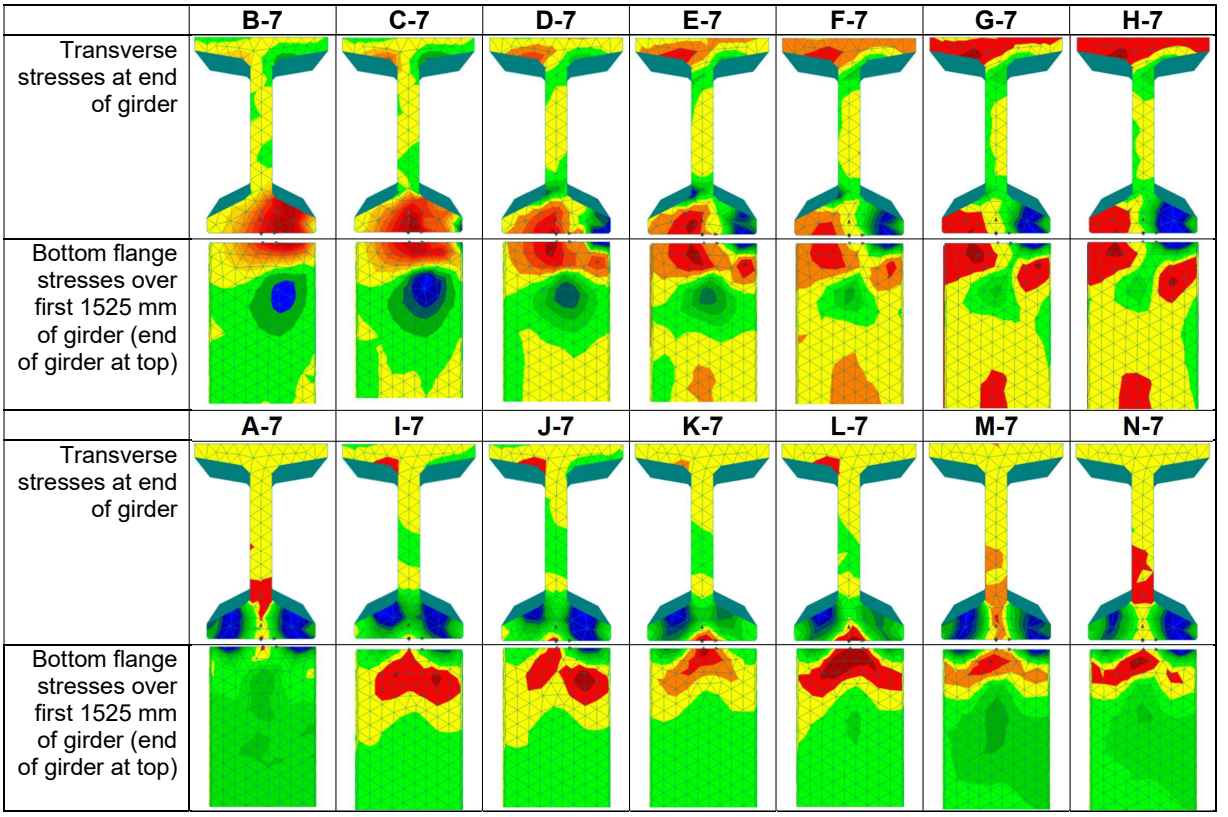

Figure 5. Transverse stress results from cases A-7 through N-7. Note: Color maps are qualitative only. Red is tension, blue is compression. Color maps vary from minimum to maximum stress in each analysis and do not represent the same stress levels in subsequent figures. 1 mm = 0.039 in.

does not occur at the vertical planes suggested by Ross; thus, the combined case that superimposes peeling and Hoyer-induced stresses is also likely an overestimation of the actual stress state.

The estimations of the values of L_t and L_z used in the analytic model (Fig. 6) are generally confirmed by the FE analysis at early stages in outside-in strand-release sequences (cases B and C) before lateral bending of the beam begins to affect behavior.

Based on these analyses, the peeling behavior hypothesized by Ross[5] is not deemed to be a significant consideration and is easily mitigated by conventional good practice strand-release sequences. Furthermore, such peeling has not been observed (to the knowledge of the authors) outside of extreme strand patterns and release sequences, such as those reported in Fig. 2 and 3.

Conclusion

Peeling stresses are not unique to heavily prestressed girders or to larger (0.7 in. [17.8 mm] diameter) strands. Shapes with wide, flat flanges exhibit large, predicted peeling stresses whereas sections with stockier flanges exhibit lower stresses overall. Peeling stresses can be mostly mitigated by partially debonding strands in the recommended pattern from the outside in.[3] Similarly, the pattern chosen for releasing or cutting strands can mitigate peeling stresses. While releasing all strands simultaneously is optimal, it is unlikely to be practical or even feasible for large prestressed components. For conventional release operations, a symmetrical top-down method should not result in significant peeling stress.

Detailing requirements for prestressed girder end regions that aim to provide adequate flange confinement and strand anchorage at the ultimate limit state[1,2] should be adequate to control peeling stresses—even those resulting from the inadvertent use of a poor release sequence.

Acknowledgment

The study reported in this paper was funded by the National Cooperative Highway Research Program (NCHRP) Project 12-109. That study is reported in full in Shahrooz et al.[10]

References

1. Harries, K. A., B. M. Shahrooz, P. Ball, T. Liu, A. Al-

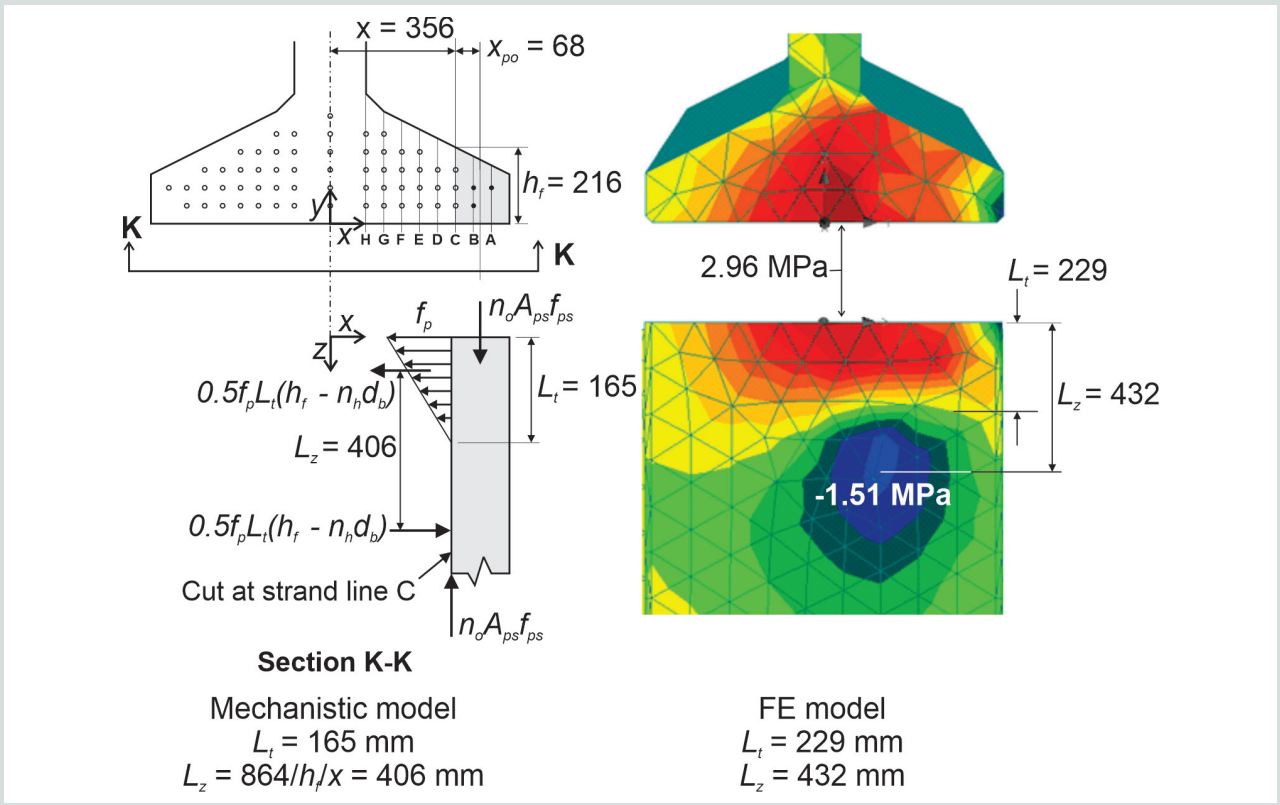

Figure 6. Visualization of peeling model from case C-7. Note: A_{ps} = area of single prestressing strand; d_b = diameter of prestressing strand; fp = maximum transverse tension stress due to peeling; f_{ps} = stress in prestressing strand; h_f = height of bottom flange; L_t = transfer length; L_z = internal resisting moment arm in the z direction; n_h = number of strands with diameter d_b along the vertical section defined by h_f; n_o = number of bonded strands outboard of the section; x = horizontal distance from the face of the web to the section considered; x_{po} = distance from the centroid of outboard strands to the vertical section defined by h_f. 1 mm = 0.0394 in.; 1 MPa = 0.145 ksi.

abdulkarim, R. A. Miller, and R. W. Castrodale. 2023. "How Long Is Long? Analytical Study of Precast, Pretensioned Concrete Girder Spans Using 0.7 in. Diameter Strand." *PCI Journal* 68 (4): 65–87. https://doi.org/10.15554/pcij68.4-02.

2. Harries, K. A., B. M. Shahrooz, B. E. Ross, P. Ball, and H. R. Hamilton. 2019. "Modeling and Detailing Pretensioned Concrete Bridge Girder End Regions Using the Strut-and-Tie Approach." *Journal of Bridge Engineering* 24 (3). https://doi.org/10.1061/(ASCE)BE.1943-5592.0001354.

3. Shahrooz, B. M., R. A. Miller, K. A. Harries, Q. Yu, and H. G. Russell. 2017. *Strand Debonding in Pretensioned Girders*. NCHRP report 849, Transportation Research Board. Washington, DC: The National Academies Press. https://doi.org/10.17226/24813.

4. Llanos, G., B. Ross, and H. R. Hamilton. 2009. *Shear Performance of Existing Prestressed Concrete Bridge Girders*. Report BD 545-56. Tallahassee: Florida Department of Transportation. https://rosap.ntl.bts.gov/view/dot/17053.

5. Ross, B. E. 2012. "Function and Design of Confinement Reinforcement in Pretensioned Concrete I-Girders." PhD diss. University of Florida. https://www.proquest.com/openview/30d687591ee26fc7498b83511335aa7f/1?pq-origsite=gscholar&cbl=18750

6. AASHTO (American Association of State Highway and Transportation Officials). 2020. *AASHTO LRFD Bridge Design Specifications*. 9th ed. Washington, DC: AASHTO.

7. Hoyer, E. 1939. *Der Stahlsaitenbeton* [Piano-String-Concrete]. Berlin, Germany: Otto Elsner.

8. Briere, V., K. A. Harries, J. Kasan, and C. Hager. 2013. "Dilation Behavior of Seven-Wire Prestressing Strand—The Hoyer Effect." *Construction and Building Materials* 40: 650–658. https://doi.org/10.1016/j.conbuildmat.2012.11.064.

9. Alabdulkarim, A., K. A. Harries, B. M. Shahrooz, R. A. Miller, and R. W. Castrodale. "Bond Characterization of 0.7-in. Diameter Prestressing Strand." *Journal of Bridge Engineering* 29 (4). https://doi.org/10.1061/JBENF2.BEENG-6586.

10. Shahrooz, B. M., R. A. Miller, K. A. Harries, and R. Castrodale. 2022. *Use of 0.7-in. Diameter Strands in Precast Pretensioned Girders*. National Cooperative Highway Research Project report 994. Washington, DC: National Academies Press. https://doi.org/10.17226/26677.

11. Oh, B. H., E. S. Kim, and Y. C. Choi. 2006. "Theoretical Analysis of Transfer Lengths in Pretensioned Prestressed Concrete Members." *Journal of Engineering Mechanics* 132 (10): 1057–1066.

Notation

A_{ps} = area of single prestressing strand

c = concrete cover provided to the center of an outermost strand

C = resisting compression

d_b = diameter of prestressing strand

d_s = stressed diameter of the prestressing strand

E_c = Young's modulus of confining concrete

E_p = Young's modulus of prestressing strand

f'_c = 28-day compressive strength of concrete

f'_{ci} = concrete compressive strength at time of prestress transfer

f_H = average transverse tension resulting from Hoyer expansion

f_p = maximum transverse tension stress due to peeling

f_{pe} = effective prestress of the prestressing strand

f_{pi} = initial prestress force

f_{ps} = stress in prestressing strand

f_{pu} = tensile strength of prestressing strand

h_f = height of bottom flange of single-webbed cross section

L_t = transfer length

L_z = internal resisting moment arm in the z direction

M = moment

n_{bh} = number of bonded strands

n_h = number of strands with diameter d_b along the vertical section defined by h_f

n_{hb} = number of bonded strands

n_o = number of bonded strands outboard of the section

p = radial pressure resulting from Hoyer effect

T = resisting tension

x = horizontal distance from the face of the web to the section considered

x_{po} = distance from the centroid of outboard strands to the vertical section defined by h_f

υ_c = Poisson's ratio for concrete

υ_p = strand dilation ratio

Appendix: Predicted peeling stresses for all cases considered

Tables A.1 through **A.6** summarize peeling stresses at all vertical sections (A through H) for all single-web sections analyzed. Table 1 in the article presents summary of peak stresses from this appendix. The tensile stress permitted by AASHTO[6] at prestress transfer is $0.50\sqrt{f'_{ci}}$ ($0.19\sqrt{f'_{ci}}$ in ksi), where f'_{ci} is concrete compressive strength at time of prestress transfer. The value for f'_{ci} was assumed to be 55 MPa (8.0 ksi); that is, tensile stresses exceeding 3.7 MPa (0.54 ksi).

Table A.1. Predicted peeling stresses for the Florida I-beam (FIB) girder

FIB girder		d_b, in.	x, mm	x_{po}, mm	h_f, mm	Maximum condition	Combined condition	
						f_p, MPa	f_H, MPa	$f_p + f_H$, MPa
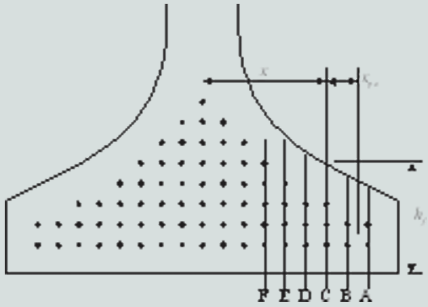	A	0.6	406	0	216	0	2.1	2.1
		0.7				0	3.2	3.2
	B	0.6	356	51	241	0.8	1.9	2.9
		0.7				1.0	2.8	4.3*
	C	0.6	305	76	267	1.7	2.6	5.0*
		0.7				2.3	4.1*	7.4*
	D	0.6	254	94	292	2.4	2.3	5.9*
		0.7				3.4	3.6	8.5*
	E	0.6	203	117	335	2.7	2.0	6.8*
		0.7				3.7	3.0	9.9*
	F	0.6	152	131	378	2.5	1.7	6.9*
		0.7				3.5	2.6	10.2*

Note: d_b = diameter of prestressing strand; f'_{ci} = concrete compressive strength at time of prestress transfer; f_H = average transverse tension resulting from Hoyer expansion; f_p = maximum transverse tension stress due to peeling; h_f =height of bottom flange; x = horizontal distance from the face of the web to the section considered; x_{po} = distance from the centroid of outboard strands to the vertical section defined by h_f. 1 mm = 0.039 in.; 1 MPa = 0.145 ksi.

*Tensile stress at prestress transfer exceeds $0.50\sqrt{f'_{ci}}$ in MPa ($0.19\sqrt{f'_{ci}}$ in ksi).

Table A.2. Predicted peeling stresses for an AASHTO Type VI girder

AASHTO Type VI girder		d_b, in.	x, mm	x_{po}, mm	h_f, mm	Maximum condition	Combined condition	
						f_p, MPa	f_H, MPa	$f_p + f_H$, MPa
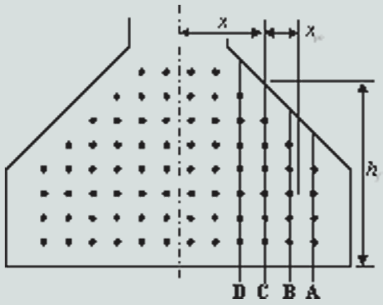	A	0.6	279	0	279	0	3.5	3.5
		0.7				0	5.4*	5.4*
	B	0.6	229	51	330	0.3	3.8*	4.2*
		0.7				0.4	5.8*	6.4*
	C	0.6	178	73	381	0.6	3.9*	4.8*
		0.7				0.8	6.1*	7.3*
	D	0.6	127	95	432	0.7	4.1*	5.1*
		0.7				1.0	6.4*	7.9*

Note: d_b = diameter of prestressing strand; f'_{ci} = concrete compressive strength at time of prestress transfer; f_H = average transverse tension resulting from Hoyer expansion; f_p = maximum transverse tension stress due to peeling; h_f =height of bottom flange; x = horizontal distance from the face of the web to the section considered; x_{po} = distance from the centroid of outboard strands to the vertical section defined by h_f. 1 mm = 0.039 in.; 1 MPa = 0.145 ksi.

*Tensile stress at prestress transfer exceeds $0.50\sqrt{f'_{ci}}$ in MPa ($0.19\sqrt{f'_{ci}}$ in ksi).

Table A.3. Predicted peeling stresses for an AASHTO bulb-tee girder

AASHTO bulb-tee girder		d_b, in.	x, mm	x_{po}, mm	h_f, mm	Maximum condition	Combined condition	
						f_p, MPa	f_H, MPa	$f_p + f_H$, MPa
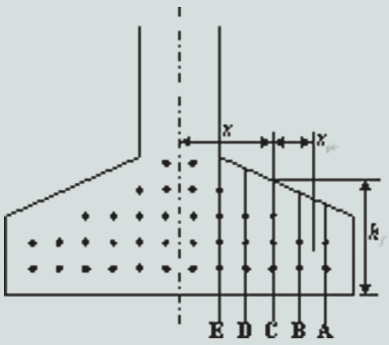	A	0.6	279	0	175	0	2.6	2.6
		0.7				0	4.0*	4.0*
	B	0.6	229	51	198	1.0	2.3	3.7
		0.7				1.4	3.4	5.4*
	C	0.6	178	76	221	2.0	3.2	6.1*
		0.7				2.8	5.0*	9.1*
	D	0.6	127	94	244	2.5	2.9	6.5*
		0.7				3.5	4.4*	9.4*
	E	0.6	76	122	267	2.3	3.7	7.1*
		0.7				3.3	5.7*	10.5*

Note: d_b = diameter of prestressing strand; f'_{ci} = concrete compressive strength at time of prestress transfer; f_H = average transverse tension resulting from Hoyer expansion; f_p = maximum transverse tension stress due to peeling; h_f =height of bottom flange; x = horizontal distance from the face of the web to the section considered; x_{po} = distance from the centroid of outboard strands to the vertical section defined by h_f. 1 mm = 0.039 in.; 1 MPa = 0.145 ksi.

*Tensile stress at prestress transfer exceeds $0.50\sqrt{f'_{ci}}$ in MPa ($0.19\sqrt{f'_{ci}}$ in ksi).

Table A.4. Predicted peeling stresses for an Ohio wide flange girder

Ohio wide flange girder		d_b, in.	x, mm	x_{po}, mm	h_f, mm	Maximum condition	Combined condition	
						f_p, MPa	f_H, MPa	$f_p + f_H$, MPa
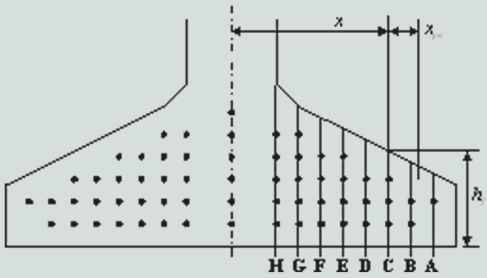	A	0.6	457	0	165	0	1.3	1.3
		0.7				0	1.9	1.9
	B	0.6	406	51	191	1.7	2.4	4.8*
		0.7				2.3	3.6	7.1*
	C	0.6	356	68	216	4.8*	3.4	10.5*
		0.7				6.9*	5.2*	15.4*
	D	0.6	305	75	241	8.1*	3.0	14.9*
		0.7				11.4*	4.5*	21.4*
	E	0.6	254	107	267	11.0*	3.7	20.0*
		0.7				15.7*	5.7*	29.0*
	F	0.6	203	125	292	12.1*	3.3	21.2*
		0.7				17.1*	5.1*	30.3*
	G	0.6	152	146	318	12.2*	3.9*	22.0*
		0.7				17.4*	6.1*	32.0*
	H	0.6	102	164	368	8.4*	3.2	15.7*
		0.7				11.9*	5.0*	22.6*

Note: d_b = diameter of prestressing strand; f'_{ci} = concrete compressive strength at time of prestress transfer; f_H = average transverse tension resulting from Hoyer expansion; f_p = maximum transverse tension stress due to peeling; h_f =height of bottom flange; x = horizontal distance from the face of the web to the section considered; x_{po} = distance from the centroid of outboard strands to the vertical section defined by h_f. 1 mm = 0.039 in.; 1 MPa = 0.145 ksi.

*Tensile stress at prestress transfer exceeds $0.50\sqrt{f'_{ci}}$ in MPa ($0.19\sqrt{f'_{ci}}$ in ksi).

Table A.5. Predicted peeling stresses for a University of Nebraska NU girder

NU girder		d_b, in.	x, mm	x_{po}, mm	h_f, mm	Maximum condition	Combined condition	
						f_p, MPa	f_H, MPa	$f_p + f_H$, MPa
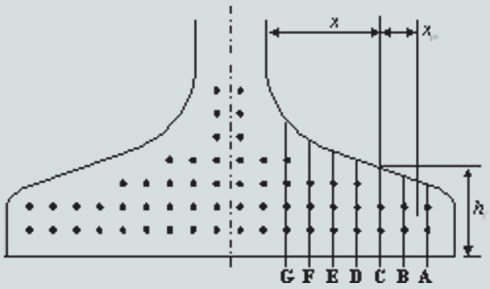	A	0.6	432	0	155	0	3.1	3.1
		0.7				0	4.7*	4.7*
	B	0.6	381	51	175	2.6	2.6	6.4*
		0.7				3.5	4.0*	9.3*
	C	0.6	330	76	196	5.2*	2.3	10.1*
		0.7				7.2*	3.5	14.3*
	D	0.6	279	102	216	7.7*	3.4	15.0*
		0.7				10.9*	5.2*	21.6*
	E	0.6	229	119	236	9.0*	3.0	16.5*
		0.7				12.8*	4.6*	23.7*
	F	0.6	178	140	254	9.2*	2.8	16.5*
		0.7				12.9*	4.1*	23.5*
	G	0.6	127	163	274	8.6*	3.6	16.5*
		0.7				12.3*	5.5*	23.9*

Note: d_b = diameter of prestressing strand; f'_{ci} = concrete compressive strength at time of prestress transfer; f_H = average transverse tension resulting from Hoyer expansion; f_p = maximum transverse tension stress due to peeling; h_f =height of bottom flange; x = horizontal distance from the face of the web to the section considered; x_{po} = distance from the centroid of outboard strands to the vertical section defined by h_f. 1 mm = 0.039 in.; 1 MPa = 0.145 ksi.

*Tensile stress at prestress transfer exceeds $0.50\sqrt{f'_{ci}}$ in MPa ($0.19\sqrt{f'_{ci}}$ in ksi).

Table A.6. Predicted peeling stresses for a Washington State Department of Transportation (WSDOT) wide flange girder

WSDOT wide flange girder		d_b, in.	x, mm	x_{po}, mm	h_f, mm	Maximum condition	Combined condition	
						f_p, MPa	f_H, MPa	$f_p + f_H$, MPa
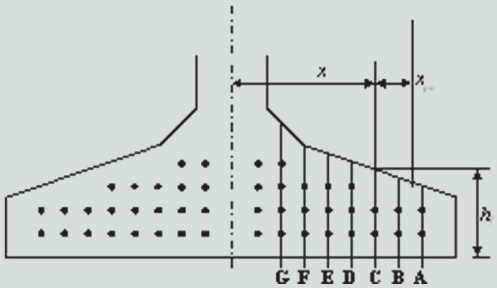	A	0.6	413	0	157	0	3.0	3.0
		0.7				0	4.6*	4.6*
	B	0.6	362	51	175	2.5	2.6	6.3*
		0.7				3.5	4.0*	9.2*
	C	0.6	311	76	193	5.2*	2.3	10.1*
		0.7				7.4*	3.6	14.3*
	D	0.6	260	102	211	7.9*	3.5	15.1*
		0.7				11.3*	5.4*	21.9*
	E	0.6	210	119	229	9.3*	3.2	16.8*
		0.7				13.2*	4.8*	24.1*
	F	0.6	159	140	246	9.4*	2.9	16.6*
		0.7				13.2*	4.4*	23.8*
	G	0.6	108	163	284	7.2*	3.4	14.0*
		0.7				10.3*	5.3*	20.3*

Note: d_b = diameter of prestressing strand; f'_{ci} = concrete compressive strength at time of prestress transfer; f_H = average transverse tension resulting from Hoyer expansion; f_p = maximum transverse tension stress due to peeling; h_f =height of bottom flange; x = horizontal distance from the face of the web to the section considered; x_{po} = distance from the centroid of outboard strands to the vertical section defined by h_f. 1 mm = 0.039 in.; 1 MPa = 0.145 ksi.

*Tensile stress at prestress transfer exceeds $0.50\sqrt{f'_{ci}}$ in MPa ($0.19\sqrt{f'_{ci}}$ in ksi).

About the authors

Kent A. Harries is a professor at the University of Pittsburgh in Pittsburgh, Pa.

Tianqiao Liu is an associate professor at Beijing University of Technology in the People's Republic of China and a former postdoctoral researcher at the University of Pittsburgh.

Bahram M. Shahrooz is a professor at the University of Cincinnati in Cincinnati, Ohio.

Richard A. Miller is a professor at the University of Cincinnati.

Reid W. Castrodale is president of Castrodale Engineering Consultants in Concord, N.C.

Abstract

Strand debonding patterns and release (prestress transfer) practices can result in significant local stresses at prestressed girder ends, which are not accounted for in design. This article presents a numerical and analytic study of various single-webbed prestressed concrete girder shapes for which large amounts of prestressing are necessitated by the use of 0.7 in. (17.8 mm) diameter strands. Shapes with wide bottom flanges are shown to potentially exhibit large stresses that effectively pry, or peel, the portions of the flanges extending from the web away from the web. Such peeling stresses can be mostly mitigated by partially debonding strands in the recommended pattern from the outside in. Similarly, releasing or cutting strands in a uniform manner mitigates peeling stresses. While releasing all strands simultaneously is optimal, it is unlikely to be practical for large prestressed components. For conventional release operations, the results presented in this article indicate that a symmetrical top-down method would not result in significant peeling stress. Moreover, prestressed girder end region detailing requirements aimed at providing adequate flange confinement and strand anchorage at the ultimate limit would be adequate to control peeling stresses, including those resulting from the inadvertent use of a poor release sequence.

Keywords

Long span, prestressing strand, pretensioned concrete.

Review policy

This paper was reviewed in accordance with the Precast/Prestressed Concrete Institute's peer-review process. The Precast/Prestressed Concrete Institute is not responsible for statements made by authors of papers in *PCI Journal*. No payment is offered.

Publishing details

This paper appears in *PCI Journal* (ISSN 0887-9672) V. 69, No. 5, September–October 2024, and can be found at https://doi.org/10.15554/pcij69.5-01. *PCI Journal* is published bimonthly by the Precast/Prestressed Concrete Institute, 8770 W. Bryn Mawr Ave., Suite 1150, Chicago, IL 60631.

Reader comments

Please address any reader comments to *PCI Journal* editor-in-chief Tom Klemens at tklemens@pci.org or Precast/Prestressed Concrete Institute, c/o *PCI Journal*, 8770 W. Bryn Mawr Ave., Suite 1150, Chicago, IL 60631.